S11-39
234146
p.9

COMBINING FRACTURE MECHANICS AND ULTRASONIC NDE TO PREDICT THE STRENGTH REMAINING IN THICK COMPOSITES SUBJECTED TO LOW-LEVEL IMPACT

Eric I. Madaras, Clarence C. Poe, and Joseph S. Heyman

NASA Langley Research Center, Hampton, Va. 23665

ABSTRACT

Predictions of the ultimate strength of damaged material have proven difficult to make. This type of prediction involves the combination of two factors: 1) an understanding of the mechanics of fracture, and 2) a method of measuring the relevant modes of damage in a non-destructive manner. The research reported here is focused upon the problem of predicting the remaining tensile strength of thick composites that were subjected to low-velocity impact damage which left no visible surface marks. This type of hidden damage can reduce the strength of thick composite materials significantly. For this research, specially fabricated thick composites were impacted using a one inch diameter ball as the indenter. These samples were non-destructively evaluated by ultrasonic through transmission and x-ray dye penetrant methods. The samples were then loaded in tension until failure. Predictions of the fracture strengths based on a fracture mechanics model combined with ultrasonic measurements generated good correlations with the actual measured fracture strengths.

I. Introduction

Thick composites are playing an increasingly important role in aerospace and aeronautical structures. Structures such as rocket motor casings and airframe components are being created with thicknesses of one inch or more. The thickness of these structures creates new difficulties in predicting their mechanical characteristics. Reliable certification of airworthiness is an important problem. A non-destructive prediction of the material's useful strength while it is in service is necessary.

Impact damage is a potentially serious problem in thick composites. Structures that employ thick composites are usually very massive. For example, a segment from NASA's space shuttle solid booster rocket motor weighs 17,900 to 57,700 lbf when empty and between 261,000 and 301,200 lbf when loaded with fuel (see figure 1). Thus each loaded rocket motor is in excess of 1,000,000 lbf. (Each composite rocket motor proposed for the Shuttle saves almost 30,000 lbf in weight over the conventional steel cased motors.) These structures must be carefully handled because the static stresses involved with lifting are significant. Motor sections can be damaged by setting them down on a hard object or bumping another structure with even a very low velocity.

Most composites fail rather catastrophically and give little indication of impending failure. Furthermore, impact damage in composites is not always visually evident. Impacts by sharp objects will leave visible scratches or puncture mark on the surface. In contrast, a blunt impacter will not leave a detectable mark for impact forces up to about 17 kips (17,000 lbs), yet the strength of the composite could be reduced by as much as 37% [1]. A blunt impacter will leave a dent or a crater for impact forces above 17 kips. In the case of a blunt impacter, the degree of damage is difficult to ascertain by standard dye penetrant radiological means because the dye is not readily taken up by the composites used in this test. Large property variations that occur in the manufacturing of composite samples make many ultrasonic techniques unreliable.

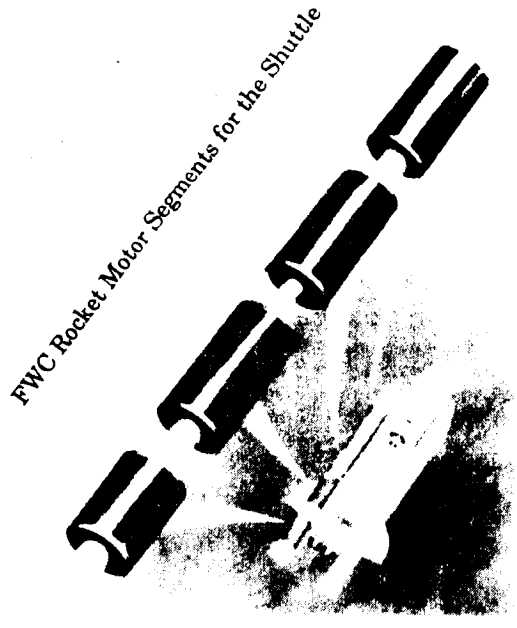

Figure 1. Proposed filament wound casing sections for the solid rocket motors to be used with the space shuttle

Two factors will be important in order to predict the failure strength of these materials: 1) accurate knowledge of the degree of damage and 2) viable fracture mechanics models for failures due to stressing of an impacted sample. This work attempts to combine these two features into a working model for predicting the tensile strength of composites with invisible impact damage.

Our approach was to employ a fracture model for predicting the fracture strength of homogeneous materials modelled with elliptical cuts. Our NDE probe used through-transmission ultrasound and an estimate of the degree of internal damage was derived from this data. The NDE results were then used as input into the fracture mechanics model to predict the fracture strength.

II. The Fracture Mechanics Model

It is predicted that at the moment of a low-velocity impact, the strains that result from compressive and shearing stresses in a thick composite are greatest just below the surface of the composite [2,3] (see figure 2a for an example of the static principle shear stresses). This implies that impacts in thick composites have a greater degree of damage internally than at the surface. In fact, there is evidence that in those samples which did not display visible damage at the surface, the surface may not have fractured in many cases [1,4]. Figure 2b is a schematic of a cross section showing what might be expected for the internal damage. Figure 2b shows a region where the fibers are broken and the matrix is fractured; which is surrounded by a region of simple matrix cracking, plus, possibly some delaminations which may occur at the bottom of the damage.

Fiber breakage is important to the load-carrying ability of these composites, and especially in the load-carrying hoop fibers. Figure 3a shows a composite with an impact damaged region. Figure 3b shows a schematic of a surface cut on a composite that is the basis of our fracture model for predicting the mode of failure. In this model, we postulate that in the vicinity of the damage, the composite is essentially disconnected across the damaged region. This is probably a reasonable approximation since the damaged matrix cannot transfer the stress loads properly to adjacent viable fibers. Thus, all the broken fibers in this region may represent a simple structure like a crack or cut. The impact model that we employed was derived for predicting the fracture from an elliptical cut or crack in a homogeneous material. This model provides an exact theoretical calculation for predicting the strength and manner in which the samples fracture [5,6].

Under tensile load, this model predicts the samples will fracture in two steps. The first step, illustrated in figure 4a, shows that the crack will extend laterally across the specimen. The depth of the crack will remain constant, with shearing at the base of the crack. The shearing

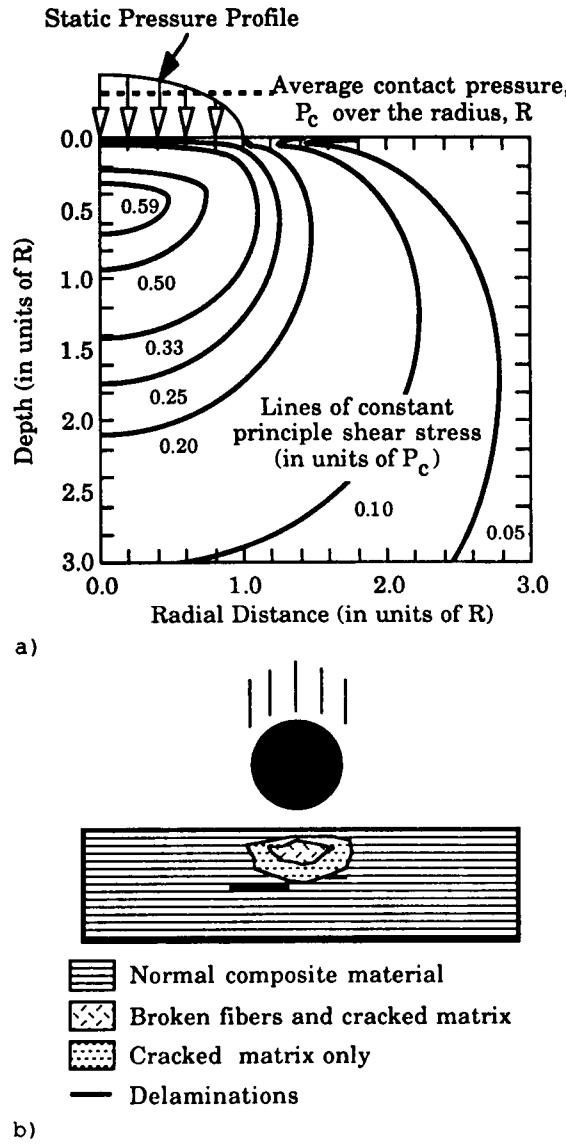

Figure 2a) Lines of constant shear stress in an infinite homogeneous half plane as a result of a hemispherical static contact force. b) Possible internal damage states in a thick composite.

failure prediction is consistent with a composites low interlaminar shear strength. This results in a thinner section with a correspondingly lower strength. The remainder of the sample will fracture as indicated in figure 4b. This theory was tested on thick FWC samples with actual elliptical cuts made in the surface. The samples did indeed fail in two steps, approximately as predicted. The measured ultimate failure strength deviated somewhat from theory. This was attributed to the possibility of out of plane

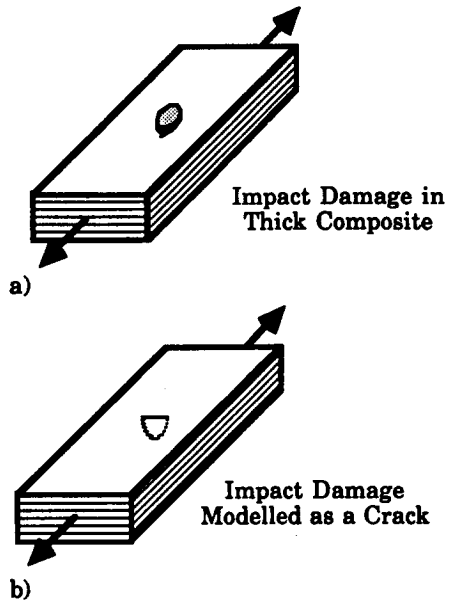

Figure 3a) A thick composite coupon showing an impact damaged site. b) The impact damaged region modelled as a crack.

bending forces that might occur in the load frame after the initial failure. Empirically, the remaining strength for the samples used in this experiment was found to approximate a power law given by

$$S = 30{,}100\ x_d^{0.278} \qquad (1)$$

where S is the strength in units of KSI and x_d is depth of the cut in inches [1]. If the hoop fibers which are along the load direction were not damaged (less than 0.19 in.), the samples would then break in the vicinity of the average ultimate strength of 50.1 KSI [4]. The empirical result, equation 1, was used to predict the remaining strength of the samples measured in this experiment.

III. Samples

In standard FWC materials the hoop fibers which are under tension are oriented circumferentially. The fiber lay-up in the samples used in this study were rotated 90° in order to best test tensile coupons in a load frame. This orientation allowed the hoop fibers to be along the axis of the cylinders and thusavoid having to test specimens in their curved direction in the load frame. The samples used in this experiment were taken from a specially wound casing manufactured with both hand layed-up plies and fiber wound plies. Fig. 5a shows a schematic of the cylinder from which the samples were derived. The cylinder was 30 inches in diameter with a thickness of 1.4 inches. This represented a cylinder that was 1/5 full scale in diameter and full scale in thickness. The length of the sample was approximately 84 inches. This

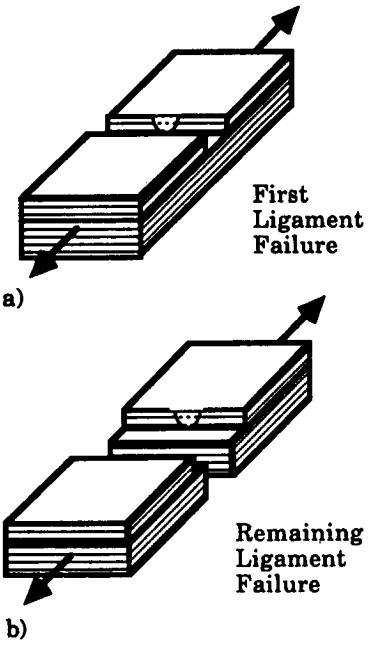

Figure 4. A representation of how a thick composite will fail. a) shows the first step and b) illustrates the remaining failure.

sample was cut into seven rings which were each 12 inches wide. The fiber lay-up directions were 0°, 56°, and -56°. Each of these rings were placed under a drop tower and impacted on the perimeter in two inch spacings with different masses and from different heights (see figure 5b). These rings were then cut up into coupons 2 inches wide by 12 inches long, each containing one impact site at its center. These coupons were then non-destructively tested by either x-ray dye penetrant methods or ultrasonic testing. Finally, the samples were loaded in tension until failure. In general, these samples failed in steps as predicted by the fracture mechanic model.

IV. X-ray Measurements

Dye penetrant x-ray photographs were made on many of the samples. These samples contained approximately 6% porosity and any dye exposed to the sides could readily be taken up, compromising the photographic measurements. Therefore, the dye was carefully exposed to the surface area just around the impact. The interesting feature about these measurements was that the dye did not enter the matrix very effectively when exposed to the impact site (see figure 6a, 7a, and 7c), indicating that the surface was not fractured. In figure 6b, a small hole was drilled into the surface at the impact site. The dye then entered the matrix region indicating the extent of the damage.

In figure 7a, the x-ray photograph shows the

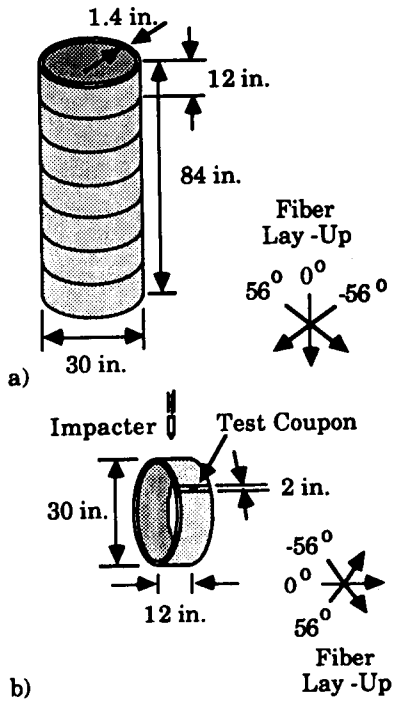

Figure 5. Illustration of the thick filament wound samples. Part a) shows the large cylinder from which smaller rings were cut and part b) illustrates the smaller rings from which the test coupons originated.

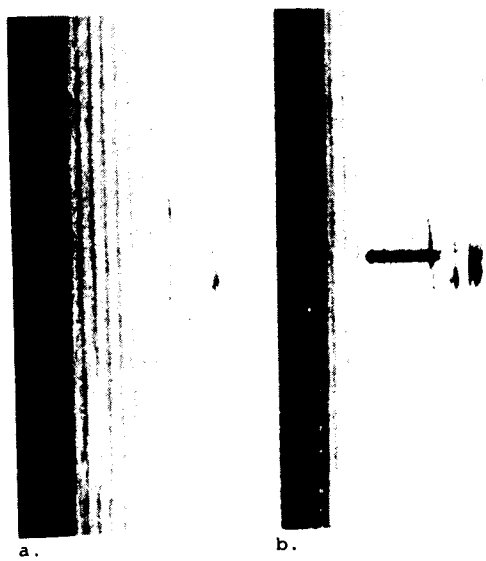

Figure 6. Dye penetration into impact damaged thick composites. Part a) shows the dye uptake into an impact damaged coupon. Part b) shows the same coupon with a small hole drilled to allow the dye to penetrate the interior.

effects of the dye penetrant method when viewed from the top; very little evidence of the damage is present. Figure 7b shows the same sample viewed from the top after it was loaded until the first failure step. Here the surface has been fractured, and the sample readily absorbs the dye. Figure 7c shows this sample from the side view, before it has been loaded. As in figure 7a, the dye is not taken up very well, and the depth of the damage is not well delineated. In contrast, figure 7d shows a side view after loading to the first failure step. Here, the sample indicates that interlaminar shearing occurs and the damage is better outlined. It is difficult to determine if the depth of damage has increased due the loading failure, but at least for testing purposes, the dye now enters the sample.

V. Ultrasonic Measurements

Many NDE techniques that are sensitive to fiber damage proved to be inadequate in these samples because of the widely varying material properties. This was a problem not only for ultrasound and x-ray radiographs, but also for techniques such as eddy currents. Figure 8 shows a close up of one of the samples. The fiber lay up is not uniform and there is significant porosity. Transmission ultrasonic measurements provided an integrating effect upon the ultrasonic response to the material properties which varied from location to location, but not upon well localized damaged material. This type of measurement, however, is not particularly sensitive to fiber breakage. We made several assumptions about the nature of the damage that enabled us to model the damage as a simple system and to circumvent the problem of detecting fiber breakage. To test this NDE model we needed to measure how well the model predicted the actual fracture strengths, based on the fracture model's equation. A second test of the model will be to impact thick samples which will be disassembled into thin layers (~2 mm thick) that can be ultrasonically measured to assess damage in each individual layer. Destructive testing of these layers will allow the ultrasonic measurements to be correlated with the damage. We have tested the first method, which is the basis of this report, and the second test of the model is being pursued.

A transmission measurement provides few parameters while these complex composites can effect those parameters in numerous ways. (Recall figure 2b which shows a schematic of the complexity of the damaged region within the composite.) This is, therefore, an indeterminate system unless we can simplify the system with the following assumptions: 1) The regions of damage can be separated into distinct uniform regions of fiber-matrix damage or matrix damage only. 2) The attenuation due to the broken fibers is linearly related to the attenuation of the fiber fractured material and the attenuation of the matrix cracked material in the following manner:

$$\alpha_{eff} = \alpha_{md} \cdot r + \alpha_{fd} \qquad (2)$$

where, α_{eff} is an "effective" attenuation of

a. b.

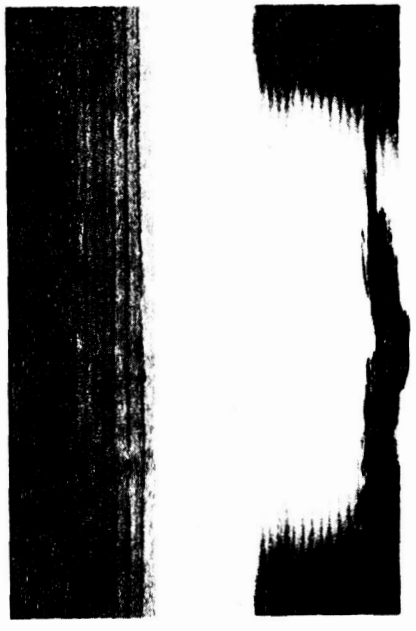

c. d.

Figure 7. A comparison of the dye uptake in an impact damaged coupon. Panel a) is the top view of dye uptake after impact, but before loading. Panel b) is the top view of the dye uptake after impact and after the first ligament failure. Panel c) is the side view of dye uptake after impact, but before loading. Panel d) is the side view of the dye uptake after impact and after the first ligament failure.

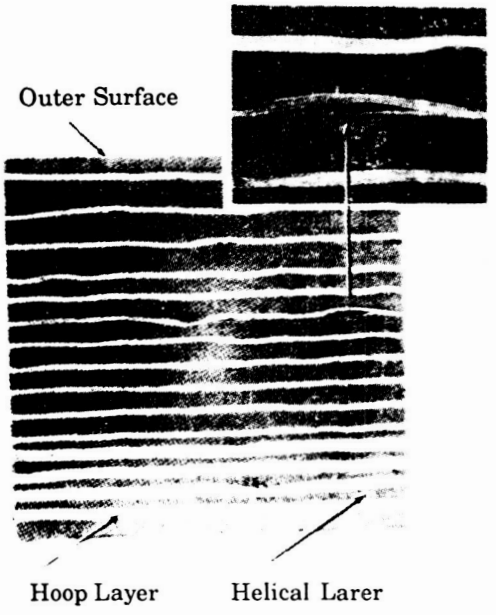

Figure 8. Photograph showing a close up of the fiber misalignment and some porosity.

damaged composite material, α_{md} is the attenuation due to matrix damaged material, r is the ratio of the matrix damaged material thickness to the fiber damaged material thickness, and α_{fd} is the attenuation of the fiber damaged material. 3) The inverse of the velocity (or slowness) is linearly related in the following manner:

$$1/v_{eff} = r/v_{md} + 1/v_{fd} \qquad (3)$$

where v_{eff} is an "effective" velocity of damaged composite material, r is as defined in equation 2, v_{md} is the velocity of matrix damaged material and v_{fd} is the velocity of the fiber damaged material. 4) Delaminations and other modes of damage are negligible. 5) The location of broken fibers range uniformly from the surface into the composite. These assumptions simplify figure 2b into figure 9. In figure 9, there are only two regions of interest; one is the normal good composite and the other an "effective" damaged composite region which is the important region related to the fiber fractured volume. Interestingly, this looks similar to the elliptical cut fracture mechanics model. These assumptions are somewhat extreme; their chief attraction is simplicity. For example, at low crack densities, attenuation is very sensitive to fiber fracture, but velocity measurements are less so [7,8]. Further research will better delineate the correct assumptions.

These assumptions result in simple algebraic relationships for the attenuation and the velocity measurements. A pulsed phase locked loop system [9] was used to determine the changes in material velocity. For these experiments, the analysis equation is:

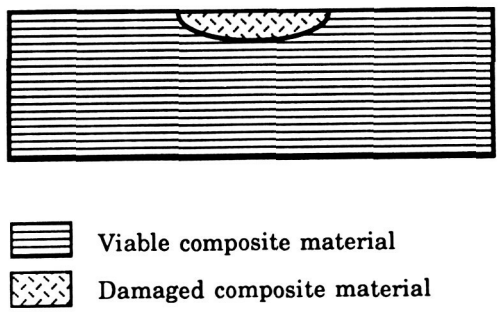

Figure 9. A schematic of the simple ultrasonic model employed in the fracture model.

$$x_d = n_\lambda (f_{ref} - f_m) \cdot (v_c \cdot v_d) / ((f_{ref} \cdot f_m) \cdot (v_c - v_d)), \quad (4)$$

where x_d is the damage thickness, n_λ is the number of wavelengths to the phase lock point, f_{ref} is the reference frequency of the phase lock loop system set in the normal composite region, f_m is the measured frequency, v_c is the velocity of normal composite, and v_{eff} is the velocity of damaged composite as defined in equation 3. For the attenuation measurements the equation is:

$$x_d = x_s (\alpha_m - \alpha_c) / (\alpha_{eff} - \alpha_c), \quad (5)$$

where x_d is again the damage thickness, x_s is the thickness of the sample, α_m is the measured attenuation, α_c is the attenuation of normal composite, and α_{eff} is the attenuation of damaged composite defined by equation 2. Most of these parameters are known or can be measured in the experiment. We can infer the correct damage cross section to use in the fracture model by knowing the appropriate attenuation and velocity of the "effective" damaged composite material .

Measurements were made near one megahertz to accommodate the high attenuation characteristics of thick composites. The transmitter was a three inch focussed 1.25 inch diameter transducer and the receiver was 0.5 inches apodized to 0.2 inch diameter to approximate a point receiver. The sample was placed so that the top surface with the impact site was at the focal zone of the transmitter. Two-dimensional scans were made in a water tank on each specimen over a 50 mm by 50 mm region centered over the impact site, using 1 mm steps. The amplitude and phase of the transmitted ultrasonic tone burst from the pulsed phase lock loop system provided attenuation and relative velocity measurements. The composite's velocity was measured by separate time of flight measurements through the samples in regions remote to the impact site. The attenuation was calibrated by measuring the signal transmitted through a water path only.

The bulk ultrasonic attenuation and velocity of normal composite material were 5-9 dB/cm for the attenuation parameter and approximately 2600 m/s at 0.9 MHz for the velocity. "Effective" attenuation of damaged composite material was extrapolated from measurements of thin impacted plates. We are presently doing experiments to verify our extrapolation, and our preliminary results tend to support our assumptions. The attenuation in composites was approximated as a linear function with frequency and characterized by intercept and slope terms. The intercept indicated contributions to the attenuation from interface losses or reflections which were frequency independent and occurred at delaminations and interfaces [10]. The slope of attenuation at the impact site predicted the bulk attenuation of damaged composite material. In thin composite material the intercept term represents a significant part of the attenuation. In thick composite materials, the bulk attenuation dominates and the intercept terms will be less significant. We assumed the intercept term to be negligible. An attenuation value of 15 dB/cm was used for damaged composite: this was a typical value measured for the slope of the attenuation at impact damage sites in similar thin composite material used in our lab. A velocity value of 2250 m/s for damaged composite material was required to match estimates of the depth of damage between attenuation and velocity measurements. Experiments are being performed to independently verify this value. This velocity value was used in equation 4 for all the impact samples.

The thickness of the damage material was predicted from equations 4 and 5 using these values for the "effective" attenuation and velocity of damaged composite. Figure 10 shows a scan image of the relative velocity. Similar views were evident for attenuation. This material displayed a large variance for the values of phase velocity and attenuation measured in the good composite material regions, and a bump that denotes the damaged region. The following algorithm was used to ignore the variability of normal regions and to determine the depth of damage. In our two-dimensional scans, the direction of loading was denoted as the y-direction. For each of the fifty x positions, we selected the minimum measured value along the y-direction scan line.

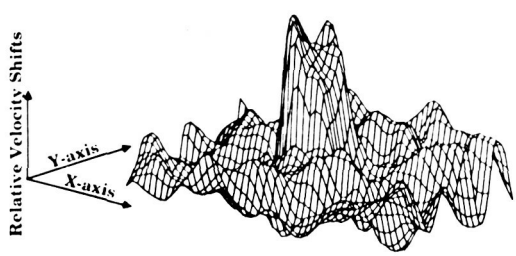

Figure 10. Wire plot showing an x-y scan image of velocity where the vertical axis represents shifts in velocity. The upwards direction indicates negative shifts in velocity.

This produced a line of data across the sample in the x-direction representing minimum frequency values for the velocity scans and minimum amplitude values for the attenuation scans. This line displayed a bump in the central region where the damage existed. By fitting a straight line through the values that were remote to the damaged values, a dividing line between normal and damaged composite was generated. For the phase velocity measurements, this value was used as f_{ref} in equation 4. In a similar manner, a line fitted to the minimum signal values of the normal regions was used for the α_c values in equation 5. The values used for f_{ref} and α_c were determined for each individual coupon. This projected the depth of damage onto two dimensions. Figure 11 shows data calculated in the above manner from velocity measurements and the result of viewing the effective depth of damage profile in the direction of the applied stress. In this figure the vertical axis shows the depth of damage into the sample, and the horizontal axis is the distance across the coupon. An elliptical shape was fitted to the damage shape and was superimposed on the depth of damage for visual reference. These damage depth values are used with the fracture strength equation to calculate the remaining strength from equation 1.

VII. Results

The remaining strength of a sample can be determined from equation 1 by knowledge of the depth of damage or, conversely, the equation can be solved for the equivalent depth of damage from the failure strength. The equivalent depth of damage is the depth of damage required in equation 1 to produce the measured strength. Figure 12 plots the X-ray measured depths of damage before loading versus the predicted equivalent depth of damage resulting from loading until fracture of

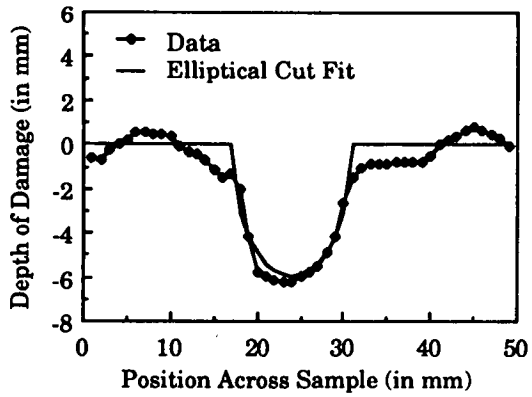

Figure 11. This is a graph of a one dimensional scan line of the depth of damage derived from a velocity scan. The tensile load direction is perpendicular to the page. The negative vertical axis represent the depth of damage into the sample.

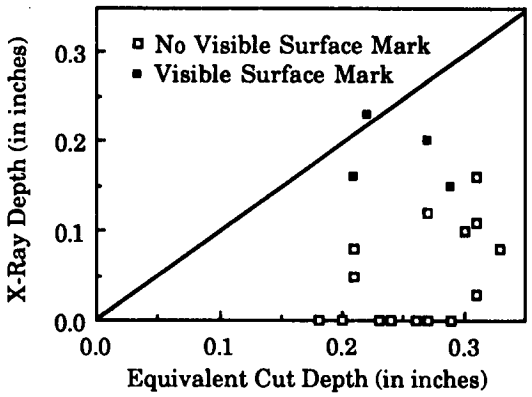

Figure 12. Depths of damage derived from X-rays compared with depths of damage derived from fracture mechanics. The solid line is the one to one correlation line

the same samples. The one-to-one correlation line is drawn for reference only. The open symbols indicate impacts that left no visible surface mark on the samples, the impacts we are concerned with in this manuscript. Also shown as solid symbols are results from four samples where the impact left a dent or visible mark. The x-ray data indicate that the depth of damage is much smaller than the equivalent depth of damage predictions for impacts that left no surface marks. In many samples, the X-ray measured depth of damage was zero. Even in the samples with a surface indication, the dye uptake indicated that the X-ray measured depth of damage was too shallow compared to the equivalent depth of damage calculations. Thus the strengths predicted from X-ray data most often resulted in overestimating the strength of the samples.

In figure 13, the ultrasonic attenuation and velocity data were used to predict the strength remaining in the samples using equation 1 and then comparing these results with the measured load levels at ultimate failure. Figure 13 shows the range of the data in units from 30 to 55 KSI. The one-to-one correlation line is drawn for reference (the solid line), as well as actual least squares linear fit to the data (the dashed line). There were no noticeable patterns to either attenuation or velocity derived data to indicate either method as superior. In the data where the samples were measured to have greater than 0.16 inches of damage depth, the samples always broke in two steps. In the cases where the estimated depth of damage was less than 0.16 inches, the samples often failed in a single step.

It is important to note that the data now scatter about the one-to-one line and that, except for four points, all the data lie within a few percent of the one-to-one correlation line. This is a very encouraging result because in eighteen

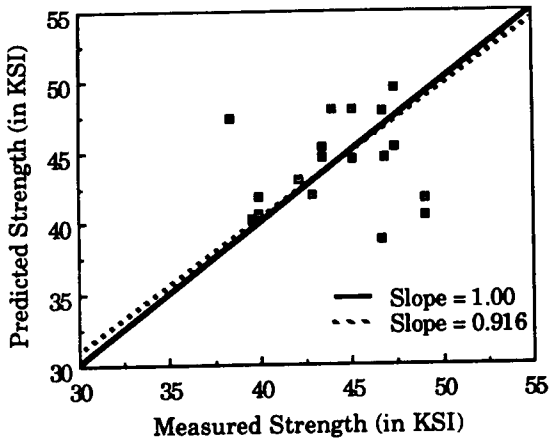

Figure 13. Predicted strengths based on the ultrasonic measurements compared with the measured fracture strengths. The solid line is the one to one correlation line, and the dashed line is the linear fit to the data.

undamaged samples, the measured strengths had variances of about 10%. Thus, the scatter in figure 13 is reasonable for the samples tested and may be due to variations in the materials.

VIII. Discussion

The goal of this set of experiments was to couple NDE measurements to fracture mechanics to predict the ultimate strength of composite samples loaded in tension. Transmission measurements of ultrasonic velocity and attenuation as well as radiographic techniques were used. The samples studied were thick FWC composites with nonvisible impact damage on the sample surface.

Radiographic x-ray measurements proved to be of little use as an NDE tool because the dye was not taken up by the samples. It was postulated that the surface sustained little or no damage so that the radio-opaque dye could not penetrate the surface. The x-ray measurements were very informative in viewing the damage after the first ligament failure. They indicated that the samples did not just fracture as a simple crack as pictured in figure 4a, but rather with many surface fractures in the region of the impact site that were oriented along the fiber lay up directions. Furthermore, the shearing in the samples was complicated, indicating shearing across ply layers and in more than one shear plane, unlike the picture shown in figure 4a. This indicated some of the limits of the fracture theory that we applied to impacted thick composites, particularly in predicting the first fracture step. The x-ray photographs do point to the fact that the samples did fracture to depths which appeared to be related to the degree of impact damage. Therefore, the remaining strength could be calculated by knowing the impact's depth of damage.

The ultrasonic measurements were made in transmission and were based on both attenuation and velocity measurements. Ultrasonic backscatter measurement techniques were tried but did not identify fiber fracture specifically, and did not generally provide reasonable resolution of the damaged regions from other regions of porosity or sample variability. By using a linear approximation to the relationship between different types of damage, a simple model was derived that could approximately relate the depth of fiber damage to the ultrasonic measurement. This model assumes that the regions of matrix only damage and regions of fiber and matrix damage scale together. Presently, there is no direct experimental support for the linear assumption. It is the simplest first approximation that can be employed. The fact that these approximations resulted in a model similar in configuration to the fracture model is attractive. Generally, fiber breakage will occur at higher damage levels than matrix fracture, and therefore, one might expect a cut-off to the relationships defined by equations 4 and 5. Similarly, either attenuation, velocity or both could exhibit a non-linear relationship between the different damage modes. The ultrasonic predictions indicated reasonably good correlations with the actual strengths, displaying about a 10% variance. This 10% variance of the strength was within the variability measured for undamaged samples, and is considered a reasonable strength predictor variance.

VIII. Conclusion

Decisions on product certification are frequently based on history of usage, such as hours of flight, or on the detection of damage by an NDE technique without knowledge of the actual remaining strength. This research afforded an interesting opportunity to combine ultrasonic techniques with fracture mechanics theory. We were able to calculate an "effective" depth of damage from ultrasonic transmission measurements. We could predict the strength of a sample under a tensile load within a 10% accuracy using fracture mechanics and this depth of damage prediction. Although the ultrasonic measurements were made in transmission, this technique should be general enough to be applicable to a single sided reflection based measurement with the possible inclusion of a diffraction correction. It is possible that this type of measurement could be coupled with the current FWC testing system, (called SUTRA), to better evaluate solid rocket motor segments.

Much work remains to be done to better define the limits of the algorithms and to develop refinements to reduce the errors. The results of this work will hopefully lead to a reliable predictor of tensile strength, including the first ligament failure point as well as the remaining ligament failure.

IX. Acknowledgements

The authors are grateful to Jeff Knutson for his

invaluable technical assistance in making the ultrasonic measurements.

X. Bibliography

1. C. C. Poe, Jr., W. Illg, and D. P. Garber, "Tension Strength of a Thick Graphite/Epoxy Laminate after Impact by a 1/2 In. Radius Impacter", NASA Technical Memorandum 87771, 1986.

2. A. E. H. Love, "The Stress Produced in a Semi-infinite Solid by Pressure on Part of the Boundary", Phil. Trans. Royal Soc. Lond. A, Vol. 228, 1929, pp. 377-420.

3. L. B. Greszczuk, "Damage in Composite Materials due to Low Velocity Impact", Impact Dynamics, John Wiley and Sons, Inc., 1982, pp. 55-94.

4. C. C. Poe, Jr., W. Illg, and D. P. Garber, "A Program to Determine the Effect of Low-Velocity Impacts on the Strength of the Filament-Wound Rocket Motor Case for the Space Shuttle", NASA Technical Memorandum 87588, Sept. 1985.

5. J. C. Newman, Jr., and I. S. Raju, "Stress-Intensity Factor Equations for Cracks in Three-Dimensional Finite Bodies". Fracture Mechanics: Fourteenth Symposium--Volume I: Theory and Analysis, ASTM STP 791, J. C. Lewis and G. Sines, Eds., American Society for Testing Materials, 1983, pp. I-238-I-265.

6. I. S. Raju, and J. C. Newman, Jr., "Stress-Intensity Factors for a Wide Range of Semi-Elliptical Surface Cracks in Finite-Thickness Plates", Engineering Fracture Mechanics, Vol. 11, No. 4, 1979, pp. 817-829.

7. J. H. Cantrell, Jr., W. P. Winfree, J. S. Heyman, and J. D. Whitcomb, "Multiparameter Characterization of Fatigue Damage in Graphite/Epoxy Composites from Ultrasonic Transmission Power Spectra", 1980 IEEE Ultrasonics Symposium Proceedings, 80CH1602, B. R. McAvoy, Ed., No. 2, pp 954-956.

8. H. I. Ringermacher, "Ultrasonic Velocity Characterization of Fatigue Damage in Graphite/Epoxy Composites", 1980 IEEE Ultrasonics Symposium Proceedings, 80CH1602, B. R. McAvoy, Ed., No. 2, pp 957-960.

9. J. S. Heyman, "Pulsed Phase Locked Loop Strain Monitor", NASA Patent Disclosure LAR 12772-1, (1980)

10. T. A. Shoup, J. G. Miller, J. S. Heyman, and W. Illg, "Ultrasonic Characterization of Fatigue and Impact Damage in Graphite Epoxy Composite Laminates", 1982 IEEE Ultrasonics Symposium Proceedings, 82CH1823-4, B. R. McAvoy, Ed., No. 2, pp 960-964.